mination. The conventional Smoluchowski approaches[11] are mute in this respect; it has been simply assumed that the intensity of illumination should be quite weak. Hence the validity of the present theory may be tested by a fluorescence quenching experiment under intense illumination.

Acknowledgement. This work was supported by a grant from the Basic Science Research Program, Ministry of Education of Korea, 1989.

References

1. J. B. Birks, Photophysics of aromatic molecules (Wiley, New York, 1970).
2. T. L. Nemzek and W. R. Ware, *J. Chem. Phys.*, **62**, 477 (1975).
3. D. P. Millar, R. J. Robbins, and A. H. Zewail, *J. Chem. Phys.*, **75**, 3649 (1981).
4. R. W. Wijnaendts van Resandt, *Chem. Phys. Letters.*, **95**, 205 (1983).
5. N. Tamai, T. Yamazaki, I. Yamazaki, and N. Mataga, *Chem. Phys. Letters.*, **120**, 24 (1985).
6. J. R. Lakowicz, M. L. Johnson, I. Gryczynski, N. Joshi, and G. Laczko, *J. Phys. Chem.*, **91**, 3277 (1987).
7. N. Periasamy, S. Doraiswamy, B. Venkataraman, and G. R. Fleming, *J. Phys. Chem.*, **89**, 4799 (1988).
8. G. C. Joshi, R. Bhatnagar, S. Doraiswamy, and N. Periasamy, *J. Phys. Chem.*, **94**, 2908 (1990).
9. F. Heisel and J. A. Miehe, *J. Chem. Phys.*, **77**, 2558 (1982).
10. J. K. Baird and S. P. Escott, *J. Chem. Phys.*, **74**, 6993 (1981).
11. S. A. Rice, Diffusion-limited reactions in comprehensive chemical kinetics, Vol. 25, eds., C. H. Bamford, C. F. H. Tipper, and R. G. Compton (Elsevier, Amsterdam, 1985).
12. G. Wilemski and M. Fixman, *J. Chem. Phys.*, **58**, 4009 (1973).
13. U. Gösele, M. Hauser, U. K. A. Klein, and R. Frey, *Chem. Phys. Letters.*, **34**, 519 (1975).
14. J. K. Baird, J. S. McCaskill, and N. H. March, *J. Chem. Phys.*, **74**, 6812 (1981).
15. R. I. Cukier, *J. Chem. Phys.*, **82**, 5457 (1985).
16. B. Stevens, *Chem. Phys. Letters.*, **134**, 519 (1987).
17. J. Najbar, *Chem. Phys.*, **120**, 367 (1988).
18. A. Szabo, *J. Phys. Chem.*, **93**, 6929 (1989).
19. H. Zhou and A. Szabo, *J. Chem. Phys.*, **92**, 3874 (1990).
20. S. Lee, M. Yang, K. J. Shin, K. Y. Choo, and D. Lee, *Chem. Phys.*, In press.
21. S. Lee and M. Karplus, *J. Chem. Phys.*, **86**, 1883 (1987).
22. S. Lee, Ph. D. Thesis, Harvard University (1986).
23. P. Sibani and J. B. Pedersen, *J. Chem Phys.*, **74**, 6934 (1981).
24. T. Förster, *Ann. Phys.*, **2**, 55 (1948).
25. M. Abramowitz and I. A. Stegun, Handbook of mathematical function (Dover, New York, 1970).

Memory of Initial States in Scattering over Attractive Potential Energy Surface for Atom-Diatom Collisions

Seung-Ho Choi and Hyung-Rae Kim*

Department of Chemistry, Hankuk University of Foreign Studies, Seoul 449-791.

Received March 22, 1991

Global and local momory functions, defined by Quack and Troe, were calculated for the rotationally inelastic collision of $O+SO(v, j)\rightarrow[O\text{--}S\text{--}O]\rightarrow O+SO(v, j')$. It is seen to decrease steadily as total energy increases. Distribution of scattering cross section over product rotational states also shows the decreasing memory of initial state as total energy is increased. These results are interpreted in terms of energy scrambling at high energy due to the availability of more phase space and also the influence of strong dynamical constraints.

Introduction

It is possible to calculate detailed state-to-state scattering cross sections for the reactions involving strongly coupled intermediate collision complexes using several well-formulated statistical theoreis[1,2] and the product state distributions for these kinds of collisions can be predicted reasonably well for some cases. Such complexes can be formed only over a deep potential well. Many neutral atom-diatom collisions are direct in nature. However a bimolecular reaction between two radical fragments of a stable triatomic molecule is known to proceed through intermediate collision complex[3,4], which is none other than highly vibrationally excited (over the dissociation limit) triatomic molecule. Therefore it would be very useful for the understanding of the reaction dynamics of a system involving the strong coupled collision complex if one could interpret the product state distribution in terms of the degree to which the initial states retain the momory of initial quantum states. This memory is closely related to the problem of redistribution of internal energy initially acquired in specific degrees of freedom[5]. The product state distribution, which is usually what is observed experimentally, can be related to the degree of ergodic state mixing that happens extensively in the strong coupling region of the complex.[6].

Even though the actual dynamics of the complex collision

and subsequent fragmentation of the complex can most accurately be described theoretically using the most up-to-date quantum scattering calculations[7], the results of the numerical calculations are not satisfactory in most cases considering the enormous labor involved in the computation. This is partly due to the unavailability of reliable *ab initio* potential energy surfaces for these complex forming reactions and partly due to the severe approximations that are usually employed to facilitate the computation in a reasonable amount of time. Therefore one usually resorts to semiclassical trajectory calculations[8], which are also time-consuming in many cases but nonetheless feasible.

On the other hand, statistical approximations can be applied to yield directly the S matrix elements without actually carrying out the dynamical calculations[9]. Even though all parts of the actual potential energy surfaces are not used, some prominent features of the surfaces are used in the computation, especially the potential energy profile along the reaction coordinate, the presence or absence of the exit channel potential barrier, or the degree of looseness of the diatomic rotor segment in the complex as the complex evolves toward the product side, namely the fragments of the complex.

Therefore we embarked on the calculation of scattering cross sections using one of the best statistical models available[1,2]. We used statistical adiabatic channel model (SACM) of Quack and Troe[2] to calculate the scattering cross sections for $O+SO \rightarrow [O\text{--}S\text{--}O] \rightarrow OS+O$. This model incorporates previously mentioned potential features in an appropriate and convenient manner so that the effects of these prominent potential characteristics can easily be investigated. Moreover, Quack and Troe presented also the concept of 'memory in scattering', which can be calculated easily, though tediously, once the cross sections and the number of total and allowed channels are known[10]. This memory function is very useful in determining how the initial information (initial quantum states, rotational and vibrational) is either carried into the product side or dissipated during the strongly interacting region, which is the collision complex.

We chose O--S--O system because very reliable analytical potential surface is known for the ground state reactions so that future quasiclassical trajectory calculations may be able to provide for the information concerning the product state distribution. The experimental data for the product state distribution or the relative recoil energy distributions are very scarce at the present time due to the radical nature of the reactants and the products. Some experimental data[11] exist for the photodissociation product state distributions but these involve some complicating factors to prohibit direct comparison with the results for the bimolecular scattering.

Theory and Computational Details

The scattering matrix elements have to be found either by dynamical calculations or by appropriate approximations inherent in statistical models. In the statistical adiabatic channel model (SACM) the statistical S matrix from (v, j) to (v', j') is given by

$$|S^{v',j',l'}_{v,j,l}(E,J)| = \begin{cases} \sigma_{v,v'}\delta_{j,j'}\delta_{l,l'} & \text{for closed channels} \\ \dfrac{1}{W(E,J)} & \text{for open channels} \end{cases} \quad (1)$$

where v, j and l are vibrational, rotational and orbital angular momentum quantum numbers, respectively, 'unprimed' referring to the reactants and 'primed' to the products. $W(E, J)$ is the number of allowed channels calculated by the use of special methods proposed by Troe and coworkers. First, channel potential curves are constructed by summing appropriate radial (along the reaction coordinate) potential curve and channel eigenvalues.

$$V_a(q) = V(q) + E_a(q) \quad (2)$$

where $V(q)$ is the electronic potential, $E_a(q)$ is the channel eigenvalue and q is the reaction coordinate. $E_a(q)$ is calculated using the correlation-interpolation method as

$$E_a(q) = E_n\, e^{-\alpha(q-q_e)} + E_p[1-e^{-\alpha(q-q_e)}] + E_c(q) \quad (3)$$

Here E_n is the eigenvalue of the collision complex at the minimum potential energy, E_p is that of product diatomic molecule and $E_c(q)$ is the centrifugal energy. E_n and E_p are given by

$$E_n = (v_n + \frac{1}{2})\varepsilon_n + (v_{bn} + \frac{1}{2})\varepsilon_{bn} + [A(q_e) - B(q_e)]K^2 \quad (4)$$

$$E_p = (v_p + \frac{1}{2})\varepsilon_p + A_p \cdot j(j+1) \quad (5)$$

where v_n and v_{bn} are the vibrational quantum numbers for the antisymmetric stretching and the bending modes of SO_2, respectively, ε_n and ε_{bn} are the corresponding vibrational quanta, $A(q_e)$ and $B(q_e)$ are the two large rotational constants of the complex at equilibrium geometry, v_p is the vibrational quantum number for the product diatom, ε_p begin its quantum, and A_p is the rotational constant of the product rotor.

The centrifugal energy is given by

$$E_c(q) = B_s(q) \cdot P(P+1) \quad (6)$$

where $B_s(q)$ is the q dependent rotational constant of the complex and can be made equal to the average of the two small rotational constants, $B(q)$ and $C(q)$, as the product atom recedes from the diatomic part, maintaining the 119.5° equilibrium angle of the bent triatomic molecule, SO_2. P is pseudo-quantum number for the centrifugal motion defined by

$$P = J \cdot e^{-\alpha(q-q_e)} + l[1-e^{-\alpha(q-q_e)}] \quad (7)$$

where J is the total angular momentum quantum number.

Omitting the vibrational degree of freedom that eventually becomes the reaction coordinate, the complex has two vibrational degrees of freedom and two rotational degrees of freedom. Since our intermediate collision complex is a near symmetric top, these rotational degrees of freedom are J, the total angular momentum quantum number, and K, the quantum number for the figure axis projection of J vector. On the product sice, v and j are the vibrational and the rotational quantum numbers of the diatomic molecule (The atom, of course, has no internal energy, except electronic energy. The O atom in our system is in the ground state, ^3P). The last term in the expression for the channel potential is due to the centrifugal motion. In order to calculate the channel energy during the dissociation or association processes (namely at q values other than q_e and infinity, q being the reaction coordinate) Quack and Troe interpolated E_n, E_p, and

$E_c(q)$ using a single parameter α. This parameter is called the looseness parameter and is a measure of the degree of loosening of the bending vibration as the reaction proceeds from the complex to the fragments. $\alpha=\infty$ corresponds to the phase space limit[1] and $\alpha=0$ corresponds to the RRKM limit[12-14]. In order to make the interpolation, the quantum numbers are classified into two categories. The oscillators whose quantum numbers and the characters are preserved during the after the scattering are called 'conserving', while those that disappear and becomes different types of oscillators or even rotors are called 'disappearing' oscillators[15,16]. The quantum numbers for the conserved oscillators remain at the same value and the quantum numbers for the disappearing oscillators change according to the correlation, which is done by matching the set of states of the complex, (v_{bm}, K), with the set of states of the products, (l, j), one by one form the bottom of the energy scale after the sets sorted on both sides. Only those states that do not violate total energy and total angular momentum conservation criteria are used in the sorting and matching. Depending on the total energy used, the number of state sets that are sorted and matched ranges from several thousands to a few tens of thousands.

Once the correlation-interpolation is done the next step is to draw the channel potential curves and determine whether each channel is allowed or forbidden. If the maximum energy of a channel potential exceeds the initial energy given, then the channel is assumed to be forbidden, while if the maximum is lower than E, then the channel is thought to be allowed. Once the S matrices are obtained (by counting $W(E, J)$ and using Eq. 1), the scattering cross sections can be calculated using the well-known expressions[17,18] for the atom-diatom inelastic or reaction cross sections, which is given as:

$$\sigma(v,\ j\to v',\ j')=\frac{\pi}{(2j+1)\ k_{vj}^{\ 3}}\sum_{J=0}^{\infty}(2J+1)\sum_{l=|J-j|}^{J+j}\sum_{l'=|J-j'|}^{J+j'}|\ \delta_{v,v'}\delta_{j,j'}\delta_{l,l'}-S^{v'j'l'}_{vjl}(E,\ J)\ |^2 \tag{8}$$

Here $k_{v,j}$ is the channel wave number given by

$$k_{v,j}^{\ 2}=2mE_t/\hbar^2$$

where m is the reduced mass for atom and diatomic fragments and E_t is the relative translational energy.

For inelastic scattering ($[v,\ j\to v',\ j']$) the cross section can be simplified as[9]

$$\sigma(v,\ j\to v',\ j')=\frac{\pi}{(2j+1)\ kv_j^{\ 2}}\sum_{J=0}^{\infty}(2J+1)\frac{W(E,\ J,\ v,\ j)\cdot W(E,\ J,\ v',\ j')}{W(E,\ J)} \tag{9}$$

where $W(E, J, v, j)$ is the number of open channels with some specified E, J, v, j.

For elastic scattering ($[v,\ j\to v,\ j]$) the cross section can be simplified as[9]

$$\sigma(v,\ j\to v,\ j)=\frac{\pi}{(2j+1)\ k_{vj}^{\ 2}}\sum_{J=0,\ W(E,\ J)\neq 0}^{\infty}(2J+1)\ W(E,\ J,\ v,\ j)\cdot\left[1+\frac{W(E,\ J,\ v,\ j)}{W(E,\ J)}\right] \tag{10}$$

Depending on which initial states are kept, the cross sections can be either 'detailed' or 'averaged'. Since we are interested in the rotational memory, the vibrational state of the reactant diatomic molcule is fixed in $v=0$, while the cross sections for different j's of the reactant rotor are calculated for all the possible final rotor j's.

Memory function is defined, by Quack and Troe, as[10]

$$\mu=\sum_{i=1}^{N}\sum_{f=1}^{N}\frac{|\ S_{fi}\ |^2}{N}\left(1+\frac{\ln|\ S_{fi}\ |^2}{\ln\ N}\right) \tag{11}$$

where S_{fi} is the S matrix for the channel where the scattering is from initial state i to final state f and N is the order of the S matrix. In the statistical model, it is assumed that all the channels that contribute to the S matrix are strongly coupled. Since the statistical S matrix is block-diagonal with one submatrix corresponding to a specific total angular momentum quantum number J and its z-component M that are allowed, the memory function can be defined for each submatrix. If the usual statistical assumption of setting the matrix element to be $1/m$ for a $m\times m$ submatrix, the memory function for each submatrix can be written as

$$\mu=1-\frac{m\cdot\ln\ m}{N\cdot\ln\ N} \tag{12}$$

Of course μ becomes $\mu(E, J)$, m becomes $W(E, J)$ and N becomes $N(E, J)$ in our case where the total energy and the total angular momentum are conserved. Taking into the different contribution by different J through appropriate weighting by the cross sections, one obtains the following function for the global measure of memory in statistical scattering[10].

$$\mu(E)=\sum_{J=0}^{\infty}(2J+1)\ \mu(E,\ J)\bar{\sigma}_J/\bar{\sigma} \tag{13}$$

where

$$\bar{\sigma}_J=\frac{\pi}{(v_m+1)(j_m+1)}\sum_{v=0}^{v_m}\sum_{j=0}^{j_m}\frac{1}{(2j+1)\ k_{vj}^{\ 2}}\sum_{v'=0}^{v_m}\sum_{j'=0}^{j_m}\sum_{l=|J-j|}^{J+j}\sum_{l'=|J-j'|}^{J+j'}|\ \delta_{v,v'}\delta_{j,j'}\delta_{l,l'}-S^{v'j'l'}_{vjl}(E,\ J)\ |^2 \tag{14}$$

and

$$\bar{\sigma}=\sum_{J=0}^{\infty}(2J+1)\,\bar{\sigma}_J \tag{15}$$

with v_m and j_m being the maximum values of v and j at E.

When one is interested in the memory of a specific internal state, it is possible to define a local memory function as follows:

$$\mu_{vj}(E)=\sum_{J=0}^{\infty}(2J+1)\ \mu_{vj}(E,\ J)\bar{\sigma}_{J,vj}/\bar{\sigma} \tag{16}$$

where

$$\bar{\sigma}_{J,vj}=\frac{\pi}{(2j+1)\ k_{vj}^{\ 2}}\sum_{v'=0}^{v_m}\sum_{j'=0}^{j_m}\sum_{l=|J-j|}^{J+j}\sum_{l'=|J-j'|}^{J+j'}|\ \delta_{v,v'}\delta_{j,j'}\delta_{l,l'}-S^{v'j'l'}_{vjl}(E,\ J)\ |^2 \tag{17}$$

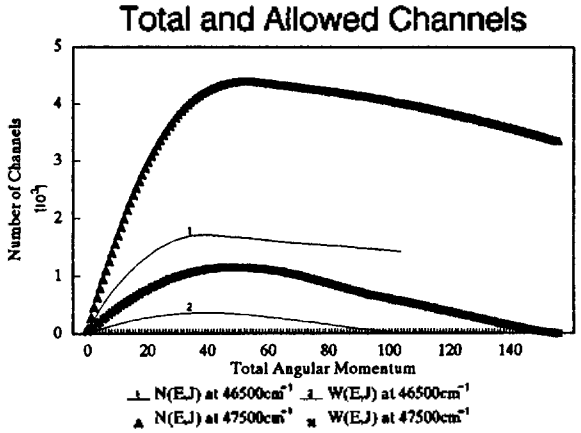

Figure 1. $N(E, J)$ and $W(E, J)$ *vs.* J at $E=46{,}500$ cm^{-1} 47,500 cm^{-1}.

and

$$\bar{\sigma}_{vj}(E)=\sum_{J=0}^{\infty}(2J+1)\ \bar{\sigma}_{Jvj} \tag{18}$$

The most important factor influencing the magnitude of memory is the ratio of $W(E, J)$ over $N(E, J)$. The number of allowed channels, $W(E, J)$, is determined by the presence of local maxima which, in turn, are formed by the dynamical constrainsts due to either the electronic potential barrier, the centrifugal barrier or other dynamical features such as the looseness parameter α or Morse parameter β in the adiabatic channel potential. Typical values of $W(E, J)$ and $N(E, J)$ are plotted against J for two different energies in Figure 1. As can be seen from the figure, $W(E, J)$ rises to a maximum at some J and falls down to zero at high J, indicating abrupt decrease of the number of allowed channels at high J. $N(E, J)$ also rises to a maximum and falls down at high J but not as fast as $W(E, J)$. Therefore it can be stated with certainty that memory of initial state will rise at high J and eventually the submatrix corresponding to a high J value will become unit matrix. Howevrr the cross sections for high J values drop quite fast to zero and the global and local memories that are appropriately weighted will be negligible after some high J value. Physically this means that as more and more channels are forbidden, they retain the memory of initial state but cross section is too small for this high degree of memory to contribute much to the global or local memory.

The detailed description and the source listing of the program are given elsewhere[19]. The program *sacms. f* was compiled and run, in a UNIX environment, on a MIPS-2030 workstation. The calculation normally takes about 20 minutes per energy. Data were collected for 8 different energies. The output includes, $\sigma(E, J)$, $\mu(E, J)$, $N(E, J)$, $W(E, J)$, $\sigma_{v,j}(E, J)$, $\mu_{v,j}(E, J)$ for five sets of (v, j), $\mu(E)$, $\sigma_{v,j\to v',j'}(E)$, $\sigma_{v,j\to v'}(E)$, where σ's are the cross sections, μ's are the memory functions, $N(E, J)$ is the total number of channels for a specific set of E and J, $W(E, J)$ is the number of allowed channels within the context of the SACM.

The spectroscopic data were taken mostly from Herzberg[20]. The potential energy profile was the reaction coordinate portion (the elongation of O atom from SO part of SO_2) of the analytical potential obtained by Murrell and coworkers[21].

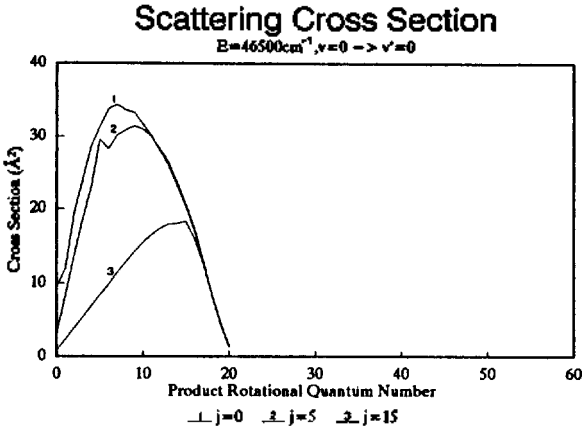

Figure 2. Rotationally inelastic cross sections. The cross sections are vibrationally elastic ($v=0\to v'=0$). Three initial j's ($j=0$, 5, 15) were used. $E=46500$ cm^{-1}.

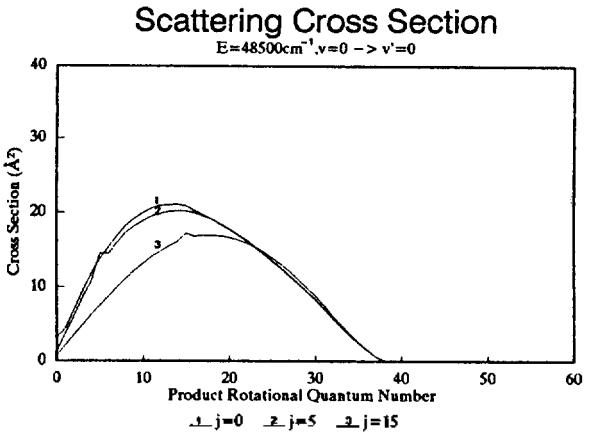

Figure 3. Same as Figure 2 except that $E=48{,}500$ cm^{-1}.

When Morse potential (where D parameter was taken from spectroscopic data and β parameter was estimated using Badger-Pauling-Johnston rule)[22] was used instead, the general behavior of the collisional event did not change much from the case when the Murrell potential was used. Only minor changes in the absolute values of the cross sections were detected by this switch of potential. This indicates quite satisfactory nature of the potential we chose because various cross sections and memory functions are expected to be a strong function of the potential characteristics.

We calculated cross sections for the rotational distributions for three differential initial j's at several initial total energies to see how the initial states are remembered by the products. We then calculated the global and local memory functions as a function of total energy.

Results

Our results are reported in two ways:

1. Product state distribution shown in Figures 2-6.
2. Global memory and local memory shown in Figures 7-9.

Product State Distributions. Starting from several different rotor j values (all at the same initial $v=0$), one can obtain the distribution of rotationally inelastic cross sec-

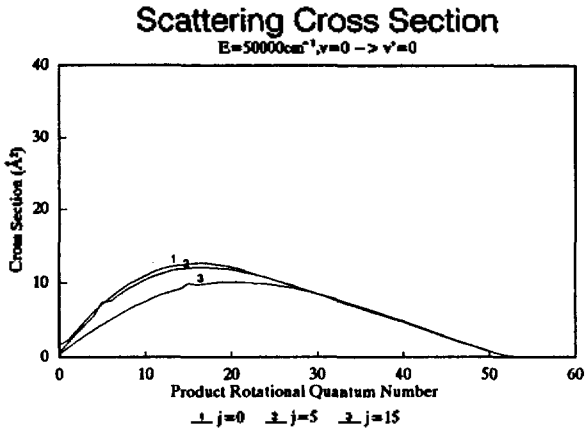

Figure 4. Same as Figure 2 except that $E=50{,}000$ cm^{-1}.

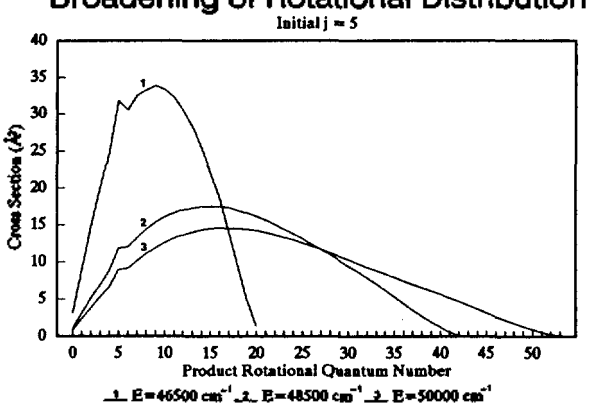

Figure 5. Broadening of the product state distribution. Initially j is fixed at 5. One can see that the widths get larger as the energy increases from 46,500 cm^{-1} to 50,000 cm^{-1}.

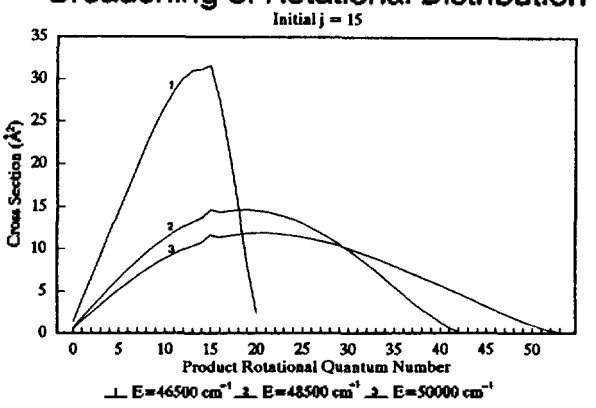

Figure 6. Same as Figure 5 except that the initial j is fixed at 15.

tions over the product rotor j values, Figure 2-4 show the results of our calculations. It is clearly seen that the distributions become similar as the total energy increases. In other words, the product state distributions get less and less dependent on the initial quantum state as the total energy (relative translational+internal) increases. At higher energy

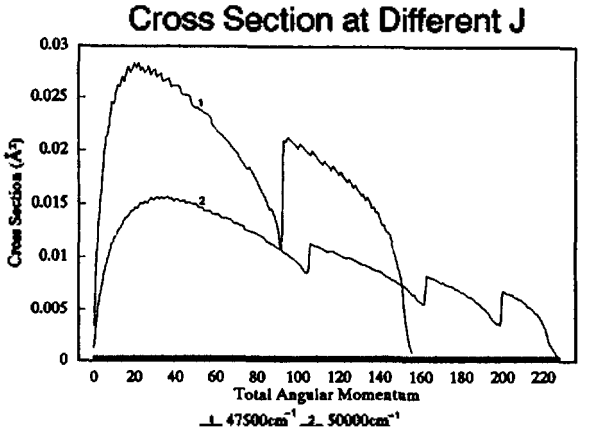

Figure 7. $\sigma(E, J)$ as a function of J for $E=47{,}500$ cm^{-1} and 50,000 cm^{-1}. As one goes from far right to left, 'kinks' appear signaling the influence of new vibrational channels.

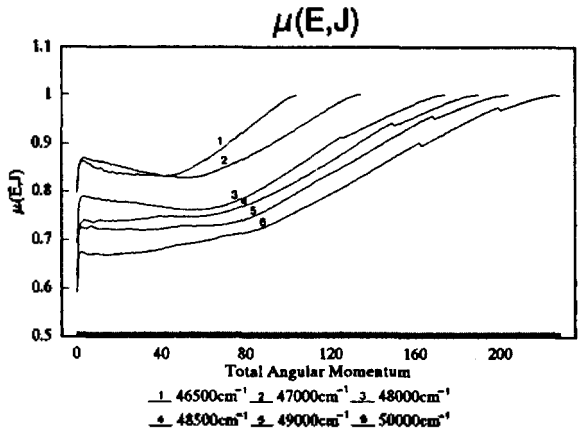

Figure 8. $\mu(E, J)$ as a function of J for several total energies. It approaches unity at the highest possible J value. Here also 'kinks" are seen for the same reason as in Figure 7.

the diatomic rotor loses a large part of its memory after the collision than at lower energy. This is due to the strongly attractive part of the potential where many internal degrees of freedom are available within the potential well and the initial energy in a specific quantum state is dissipated statistically into various degrees of freedom of the complex.

The loss of initial memory can also be seen by observing the broadening of the product rotational distribution. Since the states are strongly mixed over the attractive well, the sharp initial rotor state shows its presence by a small hump on the product distribution function as is seen in Figures 2-6. Even though the product rotors are distributed widely over the product rotor phase space, the distribution is broadened significantly as the total energy increases (Figure 5, 6). One rather peculiar thing to note is the fact the $j=0$ initial rotor state has no memory at all. As it goes through the attractive well, it forgets all its initial state (in other words, the rotor which had no rotation initially acquires rotation after it passes over the potential well).

Global and Local Memory. In order to calculate the global memory and the local memory, it is necessary to first obtain the memory and the cross section for a specific total

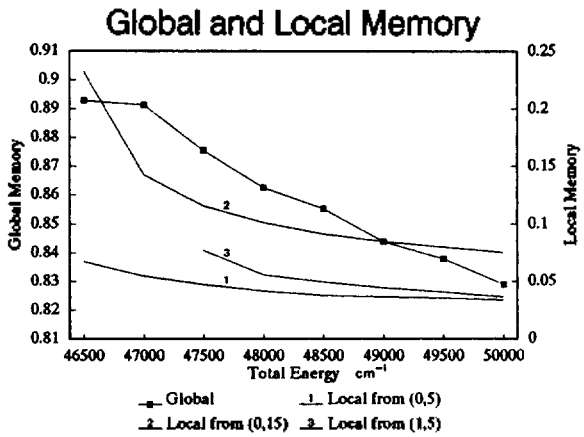

Figure 9. $\mu(E)$ and $\mu_{ij}(E)$ are plotted as a function of total energy. The local memory values should be read using the right axis.

angular momentum, denoted by $\mu(E, J)$ and $\sigma(E, J)$, respectively. Figure 7 shows $\sigma(E, J)$ for $E=47{,}500$ cm^{-1} and 50,000 cm^{-1}. The figure shows the characteristic structure due to different product channels corresponding to different vibrational states of the product diatomic molecule. The presence of different vibrational channels are felt clearly by the structure of $\sigma(E, J)$.

Figure 8 shows $\mu(E, J)$ for several different values of initial energy. Already the energy dependence is such that the memory drops as the energy increases, for most J's. Here also some kinks are seen and these are definitely due to the presence of different vibrational channels.

Figure 9 is the plot of memory (global and local) against the energy. As is expected, the global memory, $\mu(E)$, and the local memory, $\mu_{ij}(E)$, are monotonacally decreasing functions of energy. Especially, the local memory at high initial j is higher than and declines more strongly than that at low initial j. Namely the rotor with high initial rotational quantum number forgets its state faster as the energy increases than the rotor at low initial j. However as the energy increases to a high level, the decline becomes less dramatic for both initial j's.

In summary we obtained the following results.

1. The product state distributions for the scattering with different initial rotational states become closer and closer as the total energy increases.
2. The rotational distributions are broadened as the total energy increases. The effect of broadening is especially severe for the collisions of high initial j.
3. The global and local memory functions are also decreasing function of total energy. The trend for the local memory is exactly as is seen in the broadening.

Discussions

Our results clearly show the power of memory function in the interpretation of the product state distribution for the strong coupling collision. Even though we did not investigate the dependence of memory function on some characteristic features of the potential along the reaction coordinate or perpendicular to the reaction coordinate, we believe that by studying memory is is possible to reveal many interesting points concerning the nature of the collision complex. It is quite interesting to find that the memory of a statistical scattering over a very deep potential well amounts to over 0.8 (1.0 is complete memory, 0.0 is the total loss of memory). The decrease in memory for increased energy is steady but not quite as significant as expected. Our results also show that the memory of a high rotation is greater than that of a low rotation and that intial $j=0$ collision does not carry its memory over into the product side, thereby completely forgetting its initial state.

These findings clearly show the importance of the detailed dynamical features of the potential surface even for a reaction occurring *via* a strongly coupled intermediate collision complex. Therefore is should be emphasized that 'statistical' does not always mean 'completely chaotic' or 'ergodic'. The loss of memory should be more extensive for the case of phase space theory because more channels are allowed here than in the SACM because the centrifugal barrier is the only obstacle for the passage of the reacting or energy exchanging complex over to the product side. In other words the dynamical constraint is more severe for the SACM. We investigated many individual channels for the factors that affect the formmation of the channel maxima. We found that the channel eigenvalues can, in many cases, form channel maxima even without the participation of the centrifugal energy.

A plausible extension of the statistical work would be using appropriately parameterized scattering matrix elements instead of identical values of $1/W(E, J)$ for allowed channels[23]. Also the cumbersome and somewhat arbitrary single parameter correlation-interpolation method employed in the SACM could be replaced by more realistic method yet to be devised. However these possible improvements would require much more computation time, which is already significant, through not unbearable.

Of course the arguments presented in this work should be tested against reliable experimental results. In the absence of such results it would be very useful to perform quasiclassical trajectory calculations to obtain theoretical product state distributions and to compare them with statistical calculations. The quasiclassical trajectory calculations are currently under way in our laboratory. The preliminry results strongly support our statistical results.

Acknowledgement. We thank Prof. J.-K. Kim, Mr. C.-S. Kim and Mr. K.-Y. Hwang at HUFS Computing Center for their help in computation.

References

1. (a) E. E. Nikitin, *Theor. Exp. Chem.*, **1**, 144 (1965); (b) P. Pechukas and J. C. Light, *J. Chem. Phys.*, **42**, 3281 (1965); (c) P. Pechukas, J. C. Light, and C. Rankin, *J. Chem. Phys.*, **44**, 794 (1966); (d) R. A. White and J. C. Light, *J. Chem. Phys.*, **55**, 379 (1971).
2. M. Quack and J. Troe, *Ber. Bunsenges. Physik. Chem.*, **78**, 240 (1974).
3. (a) J. M. Parson and Y. T. Lee, *J. Chem. Phys.*, **56**, 4658 (1972); (b) J. M. Parson, K. Shobatake, Y. T. Lee, and S. A. Rice, *Faraday Disc. Chem. Soc.*, **55**, 344 (1973).
4. J. M. Parson, K. Shobatake, Y. T. Lee, and S. A. Rice,

J. Chem. Phys., **59**, 1402, 1416, 1427 and 1435 (1973).
5. C. S. Parmenter, *Far. Disc. Chem. Soc.*, **75**, 7 (1983).
6. D. W. Noid, M. L. Koszykowski, and R. A. Marcus, *Ann. Rev. Phys. Chem.*, **32**, 267 (1981).
7. R. B. Bernstein, *Atom-Molecular Collision Theory*, Plenum Press, New York and London, 1979.
8. P. Brumer and M. Karplus, *Far. Disc. Chem. Soc.*, **55**, 80 (1973).
9. M. Quack and J. Troe, *Ber. Bunsenges. Physik. Chem.*, **79**, 170 (1975).
10. (a) M. Quack, Dissertation, Lausanne, 1974; (b) M. Quack and J. Troe, *Ber. Bunsenges. Physik. Chem.*, **80**, 1140 (1976).
11. (a) A. Freeman, S. Yang, and R. Bersohn, *J. Chem. Phys.*, **70**, 5315 (1979); (b) H. Kanamori, J. E. Butler, K. Kawaguchi, C. Yamada, and E. Hirota, *J. Chem. Phys.*, **83**, 611 (1985); (c) M. Kawasaki, K. Kasatani, H. Sato, H. Shinohara, and N. Nishi, *Chem. Phys.*, **73**, 377 (1982); (d) H.-R. Kim, Ph.D. Dissertation, Cornell University (1984).
12. G. M. Wieder and R. A. Marcus, *J. Chem. Phys.*, **37**, 1835 (1962).
13. (a) S. A. Safron, *Long-lived collision complexes*, Thesis, Harvard University 1969; (b) S. A. Safron, N. D. Weinstein, D. R. Herschbach, and J. C. Tulley, *Chem. Phys. Letts.*, **12**, 564 (1972).
14. P. J. Dagdigian, H. W. Cruse, A. Schultz, and R. N. Zare, *J. Chem. Phys.*, **61**, 4450 (1974).
15. J. Troe, *J. Chem. Phys.*, **75**, 227 (1981).
16. J. Troe, *J. Chem. Phys.*, **79**, 6017 (1983).
17. A. M. Arthurs and A. Dalgarno, *Proc. Roy. Soc.* [London] **A256**, 540 (1960).
18. (a) R. B. Bernstein, A. Dalgarno, H. Massey, and I. C. Percival, *Proc. Roy. Soc.* [London] **A274**, 427 (1963); (b) V. F. Weisskopf, *Phys. Rev.*, **52**, 295 (1973); (c) N. F. Mott and H. S. W. Massey, *The Theory of Atomic Collisions*, Clarendon, Oxford 1965.
19. Seung-Ho Choi, MS Thesis, Hankuk University of Foreign Studies, 1991.
20. (a) G. Herzberg, *Molecular Spectra and Molecular Structure I*, D. van Nostrand, New York 1950; (b) K. P. Huber and G. Herzberg, *Molecular Spectra and Molecular Structure IV*, D. van Nostrand, New York 1979.
21. (a) S. C. Farantos, E. C. Leisegang, J. N. Murrell, and K. Sorbie, *Mol. Phys.*, **34**, 947 (1977); (b) J. N. Murrell, S. Carter, S. C. Farantos, P. Huxley, and A. J. C. Varandas, *Molecular Potential Energy Functions*, Willey, New York, 1984.
22. H. S. Johnston, *Gas Phase Reaction Theory*, Ronald Press, New York, (1966).
23. W. H. Miller, *J. Chem. Phys.*, **52**, 543 (1970).

Photoionization of N,N,N′,N′-Tetramethyl-*p*-phenylenediamine in Polar Solvents

Minyung Lee, Du-Jeon Jang, and Dongho Kim*

Spectroscopy and Color Laboratory, Korea Standards Research Institute, Taedok Science Town, Taejeon 305-606

Sun Sook Lee and Bong Hyun Boo

Department of Chemistry, Choongnam National University, Taejeon 305-746.
Received March 30, 1991

The photoinduced electron transfer reactions of N,N,N′,N′-tetramethyl-*p*-phenylenediamine (TMPD) in various polar solvents were studied by measuring time-resolved fluorescence. The temperature dependnce on the fluorescence decay rate in acetonitrile, methanol, ethanol and buthanol was carried out to obtain the activation energy and Arrehnius factor for the photoinduced electron transfer reaction. It was found that as the dielectric constant of the solvent increases, the activation energy and the reaction rate increase. This implys that the Arrehnius factor is important in controlling the photoinduced electron transfer reaction rate. In water, TMPD exists in three forms (cationic, protonated and neutral forms) due to the high dielectric constant and strong proton donating power of water. The photoinduced electron transfer reaction was found to be very fast (<50 ps) and also the long liverd component in the fluorescence decay profile attributable to the photoexcited protonated form of TMPD was observed. Probably, the reaction pathway and the reaction coordinate seem to be different depending on the solvents studied here.

Introduction

Elucidation of dynamics and mechanism of photoinduced charge or electron transfer leading to the formation of ion pair is one of the most fundamental problems in photochemical processes in polar solvents[1]. In polar solvents, an interaction between N,N,N′,N′-tetramethyl-*p*-phenylenediamine (TMPD) and solvent molecules is known to play an important role